JOURNAL OF AGRICULTURAL AND FOOD CHEMISTRY

Tentative Assignment of the Potato Serine Protease Inhibitor Group as β-II Proteins Based on Their Spectroscopic Characteristics

LAURICE POUVREAU,[†] HARRY GRUPPEN,[†,‡] GERRIT A. VAN KONINGSVELD,[†] LAMBERTUS A. M. VAN DEN BROEK,[†,‡] AND ALPHONS G. J. VORAGEN*[,†,‡]

Centre for Protein Technology TNO-WU, P.O. Box 8129, 6700 EV Wageningen, The Netherlands, and Department of Agrotechnology and Food Sciences, Laboratory of Food Chemistry, Wageningen University, Wageningen, The Netherlands

Potato serine protease inhibitor (PSPI) is the most abundant protease inhibitor group in potato tuber. The investigated PSPI isoforms have a highly similar structure at both the secondary and the tertiary level. From the results described, PSPI is classified as a β-II protein based on (1) the presence in the near-UV spectra of sharp peaks, indicating a rigid and compact protein; (2) the sharp transition from the native to the unfolded state upon heating (only 6 °C) monitored by a circular dichroism signal at 222 nm; and (3) the similarity in secondary structure to soybean trypsin inhibitor, a known β-II protein, as indicated by a similar far-UV CD spectrum and a similar amide I band in the IR spectrum. The conformation of PSPI was shown also to be stable at ambient temperature in the pH range 4−7.5. Upon lowering the pH to 3.0, some minor changes in the protein core occur, as observed from the increase of the intensity of the phenylalanine peak in the near-UV CD spectrum.

KEYWORDS: PSPI; pH stability; thermal unfolding; β-II protein

INTRODUCTION

Protease inhibitors are abundant in tubers and plant seeds (*1*). In higher plants, several gene families have been characterized, particularly those constituting the serine protease inhibitors from the Leguminosae, Solanaceae, and Graminae (*2*).

Protease inhibitors in plants seem to be involved in various processes (*3*). They have been shown to play a protectant role against insect attack and virus infection (*4*). They have also been proposed to be used as storage proteins in seeds, deduced from the fact that the maximum level of protease inhibitors coincides with the maximum level of proteolysis during germination (*5*). They also are considered to participate in the activity regulation of endogenous proteases (*6*).

In recent years, protease inhibitors have regained interest because of their potential activity in preventing carcinogenesis in a wide range of in vitro and in vivo systems (*7*). For example, serine protease inhibitors have been reported to have inhibitory effects on tumor cell growth (*8*, *9*). In addition, by increasing the level of cholecystokinin via the inhibition of trypsin, serine protease inhibitors may also be used to reduce food intake in man (*10*).

In potato, a wide range of protease inhibitors is expressed. Potato tubers contain approximately 1.5% of protein on a fresh weight basis (*11*), of which, in cv. Elkana, protease inhibitors represent up to 50% (*12*). Potato serine protease inhibitor (PSPI) was first described by Valueva and co-workers (*13*) as a dimeric serine protease inhibitor containing two active sites, one against trypsin and one against α-chymotrypsin/elastase. PSPI is the most abundant group of protease inhibitors in potato tuber (cv. Elkana) accounting for 44% of the total amount of protease inhibitors (*12*). The PSPI group consists of a group of proteins that is expressed as one polypeptide chain, which subsequently undergoes post-translational processing, during which ≈6 amino acids are cleaved off (*14*). As a result, a dimeric protein of ≈20.2 kDa is obtained with the two subunits held together by a disulfide bridge. Seven different isoforms of PSPI, with isoelectric pHs varying from 5.5 to 6.9, have been identified in potato juice (cv. Elkana) (*12*).

Protease inhibitors are important tools of nature for regulating the proteolytic activity of endogenous as well as exogenous proteases. It is, therefore, of great interest to determine which characteristic structural properties confer inhibitory activity to these proteins. Until now, the 3-D structures of only a limited amount of protease inhibitors have been determined (*15*). In this study, we determine the structural characteristics of PSPI using far- and near-UV circular dichroism and fluorescence and FTIR spectroscopy. By comparing these structural characteristics to those of more extensively studied protease inhibitors, we attempt to classify PSPI in a (sub)structural class of proteins. Proteins involved in defense mechanism, such as protease inhibitors and lectins, are known to be heat stable (*16*−*18*).

* Corresponding author. Phone: +31 317 483209. Fax: +31 317 484893. E-mail: Fons.Voragen@wur.nl.
[†] Centre for Protein Technology TNO-WU.
[‡] Wageningen University.

10.1021/jf0493932 CCC: $27.50
Published on Web 11/10/2004

Therefore, using the mentioned techniques as well as differential scanning calorimetry, the conformational stability of PSPI upon heating and at various pHs is studied.

MATERIALS AND METHODS

Preparation of PSPI Isoform Solutions.. PSPI isoforms 6.1 and 6.5 were purified as described previously (*12*, *14*) from potato juice (cv. Elkana). After purification, PSPI 6.1 and 6.5 were dialyzed at 4 °C against buffers of various pH (3.0, 4.0, 5.0, 6.0, 7.0, and 7.5) all having a calculated ionic strength of 15 mM. The buffers used were 18 mM sodium phosphate buffer (pH 3.0), 95 mM sodium acetate buffer (pH 4.0), 24 mM sodium acetate buffer (pH 5.0), 20 mM piperazine buffer (pH 6.0), 9 mM sodium phosphate buffer (pH 7.0), and 7 mM sodium phosphate buffer (pH 7.5). These buffers are denoted buffer pH 3, pH 4, pH 5, pH 6, pH 7, and pH 7.5, respectively. Subsequently, the samples were frozen in small volumes at a concentration of 0.8 mg/mL and stored at −20 °C until use.

Soybean trypsin inhibitor (STI) was purchased from Fluka (art. no.: 93618). STI (1 mg/mL) was dissolved in 9 mM sodium phosphate buffer (pH 7.0) and dialyzed against the same buffer overnight at 4 °C.

Spectroscopic Measurements. All samples were filtered through a 0.22 μm filter before spectroscopic measurements.

Far-Ultraviolet CD. Far-ultraviolet circular dichroism (far-UV CD) spectra of 0.2 mg/mL of PSPI in buffer pH 3, pH 4, pH 5, pH 6, pH 7, and pH 7.5 were recorded on a Jasco J-715 spectropolarimeter (Jasco Corp., Tokyo, Japan) at temperatures ranging from 20 to 85 °C with intervals of ∼5 °C, using a heating rate of 30 °C/h. The temperature in the sample was measured using a thermocouple wire. Starting from 20 °C, the proteins were heated to the desired temperature and equilibrated for 3 min at this temperature before the wavelength scans were recorded. Quartz cells with an optical path length of 0.1 cm were used. The scan range was 260−190 nm, the scan speed was 50 nm/min, the data interval was 0.2 nm, the bandwidth was 1.0 nm, the sensitivity was 20 mdeg, and the response time was 0.125 s. Spectra were recorded in 10-fold and averaged. Spectra were corrected by subtracting the spectrum of a protein free sample, obtained under identical conditions. Noise reduction was applied using the Jasco software. The spectra were analyzed from 240 to 190 nm to estimate the secondary structure content of the protein, using a nonlinear regression procedure (*19*). Spectra were fitted using the reference spectra of polylysine in the α-helix, β-strand, and random coil conformation (*20*) and the spectrum of β-turn structures, extracted from 24 proteins with known X-ray structure (*21*). Changes in secondary structure of PSPI during heating were also monitored by measuring the ellipticity at 222 nm.

Near-Ultraviolet CD. Near-ultraviolet circular dichroism (near-UV CD) spectra of 0.8 mg/mL PSPI, in buffer pH 3, pH 4, pH 5, pH 6, pH 7, and pH 7.5, were recorded on a Jasco J-715 spectropolarimeter (Jasco Corp., Tokyo, Japan) at various temperatures ranging from 20 to 85 °C, using a heating rate of 30 °C/h. Starting from 20 °C, the proteins were heated to the desired temperature and equilibrated for 6 min at this temperature before the wavelength scans were recorded. Spectra were recorded 30-fold and averaged. Spectra were corrected by subtracting the spectrum of a protein free sample, obtained under identical conditions. A quartz cell with an optical path length of 1.0 cm was used. The scan interval was 250−350 nm, the scan speed was 100 nm/min, the data interval was 0.2 nm, the bandwidth was 1.0 nm, the sensitivity was 20 mdeg, and the response time was 0.125 s.

Fluorescence Spectroscopy. Fluorescence spectra of 0.1 mg/mL PSPI in buffer pH 3, pH 4, pH 5, pH 6, pH 7, and pH 7.5 were recorded on a Perkin-Elmer Luminescence Spectrophotometer LS 50 B (Perkin-Elmer Corp., Boston, MA) with a pulsed Xenon source. Excitation was done at 295 nm, and the resulting emission spectrum was recorded from 305 to 405 nm, using a scan speed of 100 nm/min. Both the excitation and the emission slit were set at 3.5 nm. Spectra were recorded 3-fold and averaged. Spectra were corrected by subtracting the spectrum of a protein free sample, obtained under identical conditions.

Fourier Transformed Infrared (FTIR) Spectroscopy. Attenuated total reflection infrared (ATR-IR) spectra were recorded on a Biorad FTS 6000 spectrometer equipped with a DTGS detector (Bio Rad Laboratories Inc., Cambridge, MA). Typically, 50 mL of a 0.8 mg/mL PSPI sample in 9 mM phosphate buffer (pH 7.0) were transferred onto a germanium crystal (1 × 8 cm) and dried under air to remove excess water. Next, the crystal was placed in the light beam such that six total reflections were obtained. Spectra were accumulated at ambient temperature in the spectral region of 4000−800 cm^{-1} with a spectral resolution of 0.5 cm^{-1} prior to zero-filling and Fourier transformation, using a speed of 5 kHz and a filter of 1.2 kHz. Typically, 100 spectra were accumulated and subsequently averaged. A spectrum representing atmospheric water was subtracted from the sample spectra. All samples were prepared and analyzed at least in duplicate. Spectra were deconvoluted to analyze the underlying absorption bands using $K = 2.4$ and a full width at half-height (fwhh) of 24 cm^{-1}.

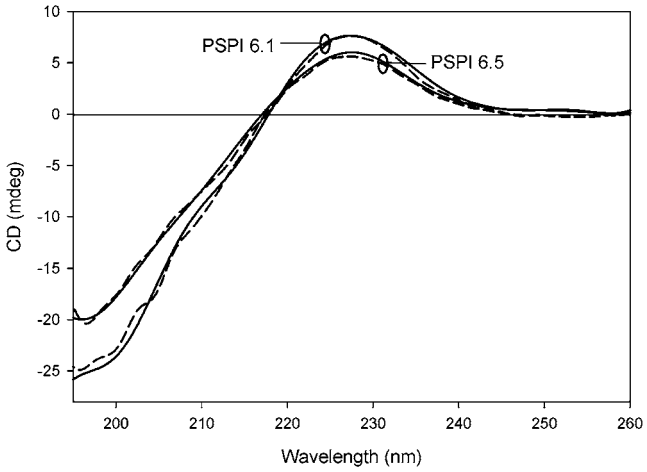

Figure 1. Far-UV CD spectra of PSPI 6.1 and 6.5 at pH 3.0 (solid line) and at pH 7.0 (dashed line), at 20 °C.

Differential Scanning Calorimetry. DSC measurements were performed on a VP-DSC microcalorimeter (MicroCal Inc., Northampton, MA). Solutions containing 0.6 mg/mL PSPI in buffer pH 3, pH 4, pH 5, pH 6, pH 7, and pH 7.5 were heated from 20 to 85 °C with a scan rate of 30 °C/h.

RESULTS

Structural Properties. PSPI 6.1 and 6.5 are the two most abundant isoforms of the PSPI group (*12*). To study possible differences in conformation between the two isoforms of PSPI at various pH values, far-UV CD, near-UV CD, and fluorescence and ATR-IR spectra of both isoforms were recorded at 20 °C.

As a typical example, **Figure 1** shows far-UV CD spectra of PSPI 6.1 and 6.5 at pH 3 and 7 at 20 °C. All spectra show a very similar pattern with a zero-crossing at about 217 nm, a minimum at 197 nm, and a maximum at 228 nm. The large similarity between the spectra indicates that the isoforms have a highly similar secondary structure in the pH range from 3 to 7.5. An estimation of the secondary structure content of PSPI isoforms, obtained by curve-fitting analysis, showed that PSPI seems to consist not only of the familiar α-helix and/or β-sheet elements, as the spectra cannot be fitted with the normal reference spectra. Especially the presence of the positive maximum at 228 nm, which cannot be ascribed to any of the known elements of secondary structure, impairs this curve fitting analysis.

Near-UV CD spectra can be used for estimating interactions of aromatic side chains with other groups such as side chain amide and carboxylate groups and peptide main chain bonds and therefore are applicable as a measure for the local tertiary structure of a protein (*22*). As a typical example, **Figure 2** shows the near-UV CD spectra of PSPI 6.1 at pH 3 and 7. Similar results were obtained at pH 3 and 7 for PSPI 6.5. The spectra

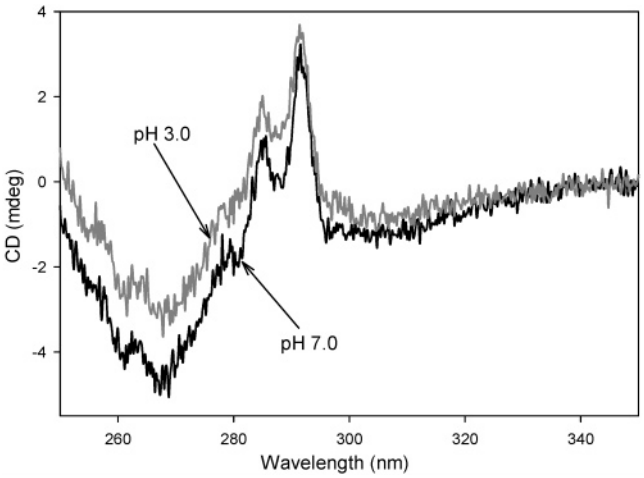

Figure 2. Near UV CD spectra of PSPI 6.1 at pH 3.0 (gray) and pH 7.0 (black) at 20 °C.

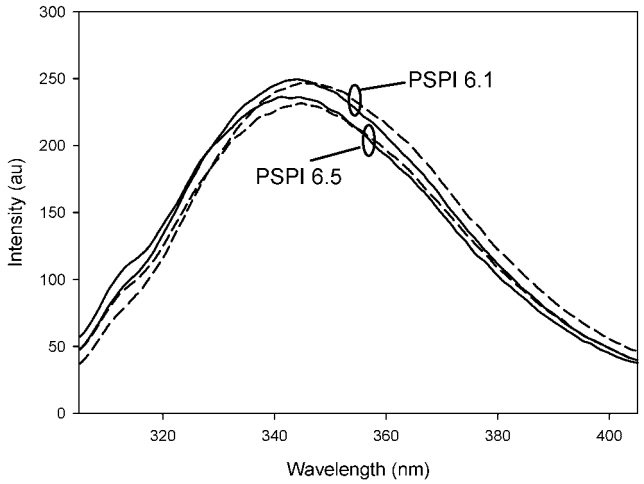

Figure 3. Tryptophan fluorescence spectra of PSPI 6.1 and 6.5 at pH 3.0 (solid line) and at pH 7.0 (dashed line) at 20 °C.

for both PSPI isoforms show extremes at 292, 285, and around 268 nm. The remarkable sharpness of the peaks at 285 and 292 nm indicates a compact rigid protein structure. The peak at 292 nm points to the presence of tryptophan residues, whereas the peaks at 285 and 268 nm indicate the presence of tyrosyl and phenylalanyl residues, respectively. These results are in accordance with the amino acid sequence of PSPI (*14*), which shows the presence of three tryptophan, seven tyrosyl, and ten phenylalanyl residues. No changes in the wavelength and the intensity of the peaks could be observed between pH 4 and 7.5 for both PSPI 6.5 and 6.1 (data not shown), indicating the absence of significant changes in the tertiary structure in this pH range. At pH 3 (**Figure 2**), a higher absolute intensity at 268 nm can be observed for both isoforms when compared to the spectra at higher pH values. This could indicate that the protein core, where the phenylalanyl residues are most frequently located, has become more compact.

Fluorescence spectroscopy provides information about the polarity of the environment of tryptophan and tyrosine residues (i.e., about the solvent accessibility of these residues). Fluorescence spectroscopy is, therefore, sensitive to local conformational changes at a tertiary level of folding (*23*). As typical examples, **Figure 3** shows the emission spectra at pH 3 and 7 for both PSPI isoforms. Within the pH range 4−7.5, the emission spectra for both isoforms remained unchanged and showed a maximum at 347 nm. This emission maximum

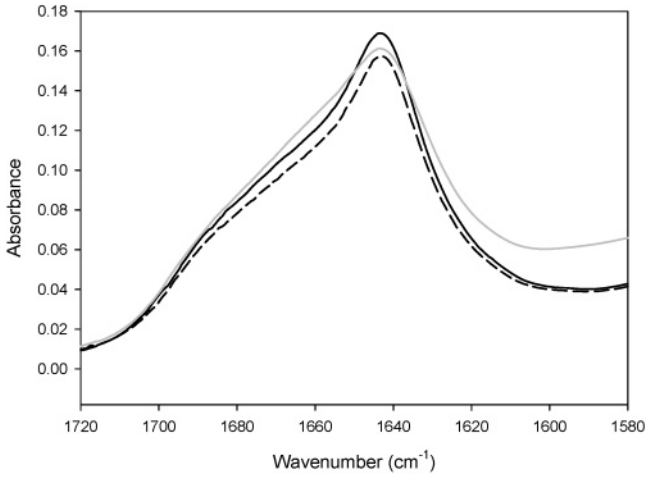

Figure 4. Amide I band of the ATR-IR spectra of PSPI 6.1 (solid line), PSPI 6.5 (dashed line), and STI (gray line) at pH 7.0 at 20 °C.

wavelength indicates that the tryptophan residues are in a nonpolar environment. The form and intensity of the emission spectra of both isoforms remained identical at pH 3, but the emission maximum had shifted 4 nm to a lower wavelength as compared to the spectra at pH ≥4. This indicates that at pH 3 the environment of at least one tryptophan residue present in PSPI (*14*) has become even less polar than at pH 4 to 7.5 and that it thus seems that the protein has become more compact.

Infrared spectroscopy is another method to investigate protein secondary structure and is based on molecular vibration of specific bonds, such as the C═O vibrations in the amide I band (1600−1700 cm^{-1}). Therefore, FTIR spectroscopycan give information on the secondary structure (*24*).

Figure 4 shows the amide I band of the infrared spectra of both PSPI isoforms and the Kunitz-type soybean trypsin inhibitor (STI), of which the X-ray structure has revealed that it contains approximately 2% α-helix, 38% β-sheet, 23% β-turn, and 37% unordered structure (*25*, *26*). The spectra indicate that there is a high degree of similarity in secondary structure between STI and the PSPI isoforms. Deconvolution of the ATR-IR spectra revealed the presence of a major band at 1642 cm^{-1}, which indicates the presence of both unordered structure and short β-sheets (*27*). Other deconvoluted bands at 1689 and 1624 cm^{-1} and at 1672 and 1662 cm^{-1} can be observed indicating the presence of β-sheets and turns, respectively, (*27*). The intensity of these bands shows that STI is somewhat richer in β-sheet and especially β-turns than PSPI.

Thermal Stability. *Secondary Structure.* As a typical example, far-UV CD spectra of PSPI 6.5 at pH 4 at various temperatures are shown in **Figure 5**. Similar results were obtained at the other pH values studied, for both isoforms upon heating. No changes in intensity occurred up to 55 °C. With increasing temperature above 55 °C, the absolute intensities at 196 and at 228 nm decreased, and the intensities were inverted. The spectral changes in **Figure 5** occurred with a clear isodichroic point at 208 nm. The existence of this point suggests that this transition may proceed essentially as a two-state process (*28*). The isodichroic point was present at all pHs and seemed not to vary with pH (207.5−208.5 nm, data not shown).

Figure 6 shows the ellipticity of PSPI 6.1 (**A**) and PSPI 6.5 (**B**) at 222 nm as a function of temperature at pH 3−7. It can be seen that the shape of the thermal unfolding curves is very similar. At pH 5 and 6, the thermal unfolding curves showed smaller transition amplitudes than at the other pH values. These differences can be explained by the fact that at these pH values

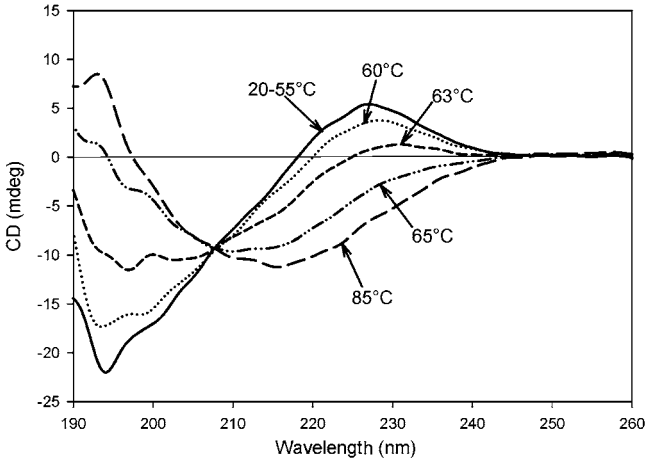

Figure 5. Far-UV CD spectra of PSPI 6.5 at pH 4.0 at various temperatures.

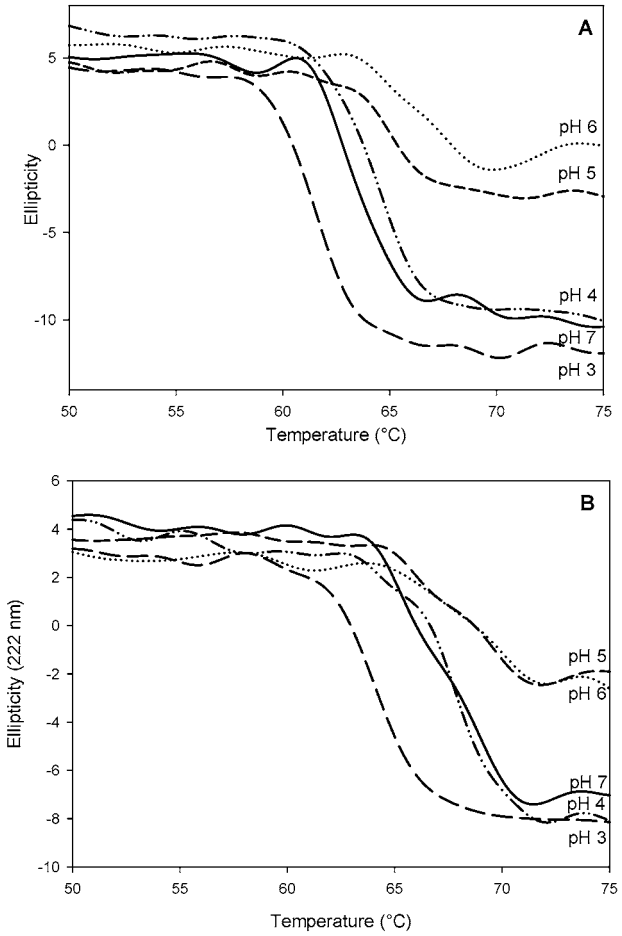

Figure 6. Thermal unfolding of curves of PSPI 6.1 (**A**) and PSPI 6.5 (**B**) at various pH values monitored by the CD signal at 222 nm.

aggregation and/or precipitation may have taken place, making the estimation of the midpoint unreliable. Nevertheless, it can be observed that at these pH values the changes in ellipticity at 222 nm occur at higher temperatures than at the other pH values. It thus seems that PSPI 6.1 and 6.5 are more thermostably close to their isoelectric pH than at other pH values. The ellipticity at 222 nm for PSPI 6.1 at, for example, pH 4 showed changes between 61.5 and 67.2 °C with a midpoint at 64.2 °C, whereas, in the case of PSPI 6.5, the changes occurred between 65.3 and 71.1 °C with a midpoint at 67.8 °C. From these data, it can be concluded that PSPI 6.5 is at all pH values more heat stable

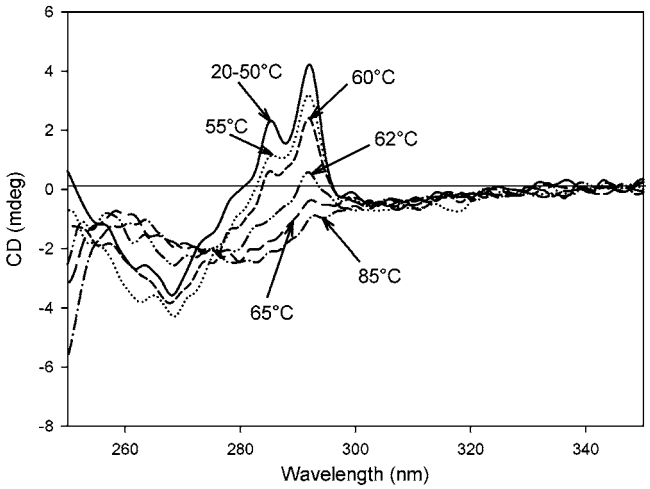

Figure 7. Near-UV CD spectra of PSPI at pH 4.0 and at various temperatures.

than PSPI 6.1 and that the difference in transition midpoint remains constant (3 and 3.5 °C). It is remarkable that the temperature range in which the changes in secondary structure in PSPI take place is very narrow (only about 6 °C), in the pH range 3−7.5.

Tertiary Structure. In **Figure 7,** near-UV CD spectra of PSPI 6.1 at pH 4 at various temperatures are shown, as typical examples. Increasing the temperature from 20 to 50 °C did not cause significant changes. Between 50 and 55 °C, a clear decrease of the peaks at 285 and 292 nm was observed. The peak at 268 nm showed an increase in absolute intensity between 50 and 55 °C, probably indicating that the core of the protein had become more compact in this temperature range. Between 60 and 62 °C, a decrease in the absolute intensity at 268 nm was observed, while at 85 °C all three peaks had disappeared. These results imply that the surroundings of the tryptophan and tyrosine residues are more heat sensitive than those of the phenylalanyl residues. The tryptophan and tyrosine residues are thus likely to be located more at the outside of the protein than the phenylalanyl residues. It can be noticed that, although at pH 3 (20 °C) the near-UV CD spectrum of PSPI was different from that at pH ≥4, PSPI unfolds at pH 3 in a similar way as at pH 4. Therefore, no effect of pH on the thermal unfolding of the tertiary structure of PSPI was observed in the pH range 3−7.5.

DSC is an additional way to study the thermal unfolding of proteins (*29*). The DSC profiles of PSPI 6.1 and 6.5 showed one symmetric peak at all pH values (**Figure 8**), except at pH 3 for PSPI 6.5 where an asymmetric peak was observed. The variation in transition temperature with pH is shown in **Figure 9**. The endothermic peak of PSPI 6.5 is always smaller in amplitude and broader than that of PSPI 6.1 (**Figure 8**). The denaturation enthalpy of PSPI 6.5 is higher than that of PSPI 6.1 in the pH range of 3−5 but becomes smaller than that of PSPI 6.1 at pH ≥7 (**Figure 9**). The calorimetric enthalpies of unfolding of PSPI 6.1 and 6.5 vary between 360 and 300 kJ/mol in the pH range 3−7.5. Similar to the data obtained from far-UV CD experiments, the transition temperatures of both PSPI 6.1 and 6.5 are highest around pH 6 and decrease when deviating from this pH (**Figure 9**). The transition temperature of PSPI 6.5 is always higher than that of PSPI 6.1 (**Figure 9**). Transition temperatures for PSPI 6.1 vary between 62 °C (pH 3) and 65 °C (pH 6), whereas those for PSPI 6.5 vary between 64 °C (pH 3) and 69 °C (pH 5 and 6). The differences in transition temperatures as observed with CD and DSC at pH 3,

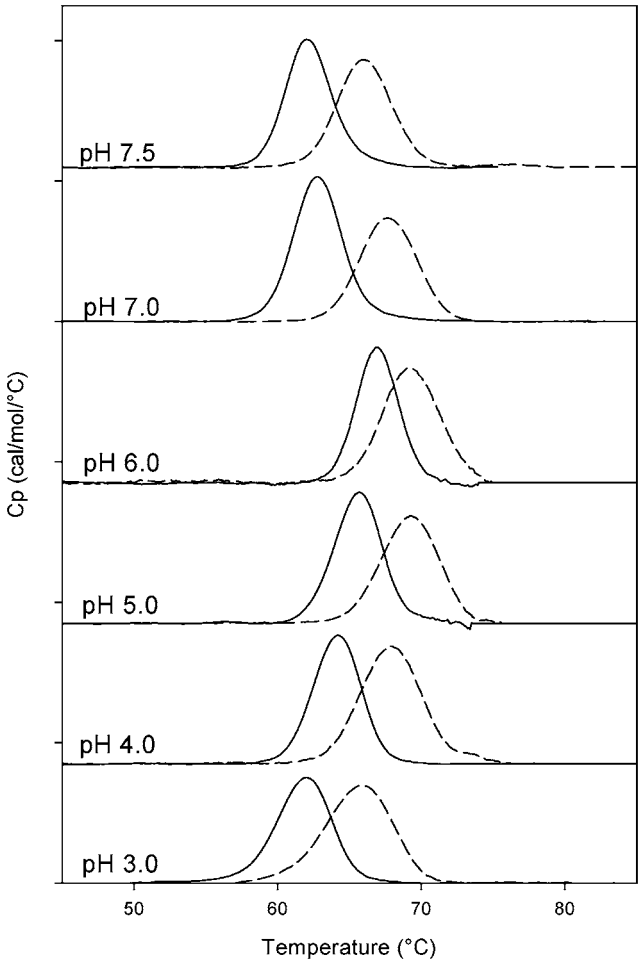

Figure 8. DSC thermograms of PSPI 6.1 (solid lines) and PSPI 6.5 (dashed lines).

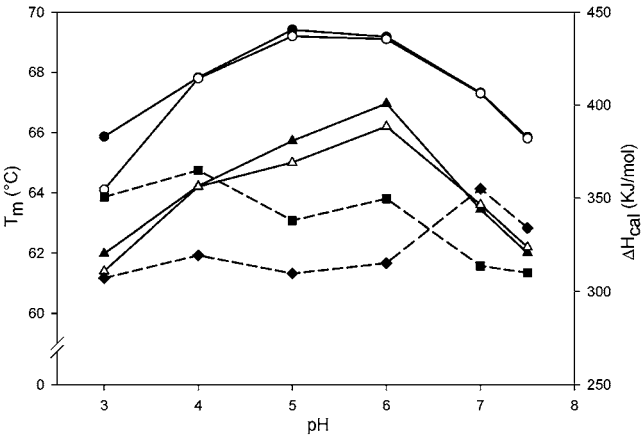

Figure 9. Transition temperatures from far UV CD (white) and DSC (black) measurements for PSPI 6.1 (▲) and PSPI 6.5 (●) and ΔH_{cal} for PSPI 6.1 (◆) and PSPI 6.5 (■), as a function of pH.

5, and 6 can be explained by the fact that at these pH values aggregation and/or precipitation may have taken place, making the estimation of the midpoint, obtained from the CD thermal unfolding curves, unreliable.

DISCUSSION

Effect of pH on the Thermal Stability of PSPI. Because of the presence of a constant isodichroic point for both isoforms at all pH values (**Figure 4**) and the similarity of the thermal unfolding curves (**Figure 5**), it can be concluded that the PSPI isoforms are almost identical and unfold via a highly similar pathway.

PSPI, at ambient temperature, did not show any variations in secondary structure in the pH range 3−7.5. At pH 3, in comparison to pH 4−7.5, small changes in the tertiary structure of PSPI did occur, which indicate that the core of the protein is somewhat more compact at this pH. Therefore, the structure of PSPI seems to be very stable against variation in pH. Furthermore, the calorimetric enthalpy (ΔH_{cal}) of PSPI 6.1 and 6.5 varies only between 300 and 350 kJ/mol (approximately 15 J/g) in the pH range 3−7.5. Experiments performed with a mixture of potato protease inhibitors showed a similar calorimetric enthalpy (approximately 19 J/g) (*30*). The thermodynamic stability of globular proteins is usually significantly affected by the pH (*31*). Bovine serum albumin showed similar variations in transition temperature as PSPI in the pH range 3−7.5. However, its ΔH_{cal} varied from 155 to 850 kJ/mol in the same pH range (*32*). Contrastingly, the α-amylase inhibitor tendimast showed a constant ΔH_{cal} in the pH range 3−7.5, whereas the variation in its transition temperature was >15 °C (*33*). For PSPI, this variation is only 4 °C over the same pH range. The results obtained and the comparison made previously clearly show the high conformational stability of PSPI in a wide pH range.

This high stability of PSPI isoforms in a broad pH range is in agreement with data previously obtained for other Kunitz-type inhibitors, such as STI (*34*), *Schizolobium parahyba* chymotrypsin inhibitor (*35*), *Erythrina caffra* trypsin inhibitor (*36*), and a chymotrypsin inhibitor from winged bean seeds (*37*). It should also be noticed that these inhibitors, as well as PSPI isoforms, all showed a sharp transition upon thermal unfolding (*34*, *38*, *39*).

In contrast to those of the PSPI isoforms, DSC curves of other Kunitz-type inhibitors showed only one endothermic asymmetric peak at various pH (*36*, *40*). More interestingly, a rescanning of the heated samples after cooling revealed that the unfolding was quantitatively reversible (*36*, *40*) while less than 5% of reversibility was observed for PSPI (data not shown). Therefore, even though Kunitz-type inhibitors share approximately 20% of their amino acid sequence, major differences exist in their thermal unfolding behavior.

Assignment of PSPI as a β-II Protein. The far-UV CD spectra of PSPI isoforms are very unusual showing extremes at 197 and 228 nm. A minimum around 200 nm has been observed in two different classes of proteins: β-II proteins and unstructured proteins (*41*). The β-II proteins are a subclass of the all-β proteins (*42*), indicating that most of the amino acid residues are predominantly involved in β-sheets and/or β-turns. In β-II proteins, most amino acid residues are involved in irregular β-sheets. The β-sheet does not have a plane extended structure but is distorted.

The far-UV CD spectra of β-II proteins resemble those of unfolded proteins in showing a minimum around 200 nm. The β-II proteins have two features that are absent for unstructured proteins. These two features can, therefore, be a tool to distinguish them. First, β-II proteins show sharp peaks in the near-UV region due to the compact structure of these proteins (*43*), even though the far-UV CD spectra resemble those of unordered protein. Second, the CD ellipticities, both in the far and in the near-UV region, of these compact and rigid proteins encompass a sharp transition upon thermal denaturation, whereas those of an unordered form usually change linearly with increasing temperature (*43*). PSPI shows, at ambient tempera-

ture, a far-UV CD spectrum resembling that of unordered proteins, with a minimum at 197 nm, and a near-UV CD spectrum with sharp peaks. Furthermore, the CD thermal unfolding curves show a sharp transition, suggesting that the changes in secondary structure occurred in a small temperature range (6 °C) (*44*). These results strongly indicate that the PSPI group is a β-II protein.

Soybean trypsin inhibitor (STI) is a well-known example of a β-II protein (*45*). Similar to PSPI, STI belongs to the Kunitz-type of protease inhibitors. STI and PSPI have a number of conserved amino acid residues in common (≈30% sequence homology), and they have a similar molecular mass (≈ 20 kDa). The far-UV CD spectrum of STI also shows a minimum at 200 nm, characteristic of the β-II proteins. Moreover, the far-UV CD spectrum of STI shows a maximum at 228 nm (*43*). STI does not contain helical parts, and most of its amino acid residues are involved in irregular β-sheet parts (*45*). The high similarity between the far-UV CD and ATR-IR spectra of PSPI and those of STI (*39*) are additional indications that the PSPI group belongs to the β-II protein subclass.

The positive maximum at 220−230 nm in the far-UV CD spectra of STI and PSPI has also been observed for many other proteases inhibitors (*46*, *47*), such as, for example, sporamin, α-amylase/subtilisin inhibitor, both Kunitz-type inhibitors (*48*, *49*), and *Erythrina* trypsin inhibitor, a known β-II protein (*50*, *51*). Therefore, it seems that the maximum at 220−230 nm in the far-UV CD spectrum is a characteristic of protease inhibitors of the β-II subclass.

Interestingly, many protease inhibitors of which the 3-D structure is known (small or large molecular weight) belong to the all-β protein class, of which the β-II proteins are a subclass. This may indicate that the presence of β-sheets is of importance for the stability of these proteins and allows the presence of stable loops at the outside of these proteins.

ABBREVIATIONS USED

PSPI, potato serine protease inhibitor; STI, soybean trypsin inhibitor.

LITERATURE CITED

(1) Ryan, C. A.; Hass, G. M.; Kuhn, R. W. Purification and properties of a carboxypeptidase inhibitor from potatoes. *J. Biol. Chem.* **1974**, *249*, 5495−5499.

(2) Garcia-Olmeda, F.; Sakedo, G.; Sanchez-Monge, R.; Gomez, L.; Royo, J.; Carbonero, P. Plant proteinaceous inhibitors of proteinases. *Oxford Survey Plant Cell Mol. Biol.* **1987**, *4*, 275−334.

(3) McManus, M. T.; Ryan, S.; Laing, W. A. The functions of proteinase inhibitors in seeds. *Seed Symp.* **1999**, 3−13.

(4) Bergey, D. R.; Howe, G. A.; Ryan, C. A. Polypeptide signaling for plant defensive genes exhibits analogies to defense signaling in animals. *Proc. Natl. Acad. Sci. U.S.A.* **1996**, *93*, 12053−12058.

(5) Ambekar, S. S.; Patil, S. C.; Giri, A. P.; Kachole, M. S. Proteinaceous inhibitors of trypsin and of amylases in developing and germinating seeds of pigeon pea (*Cajanus caja* (L) Millsp). *J. Sci. Food Agric.* **1996**, *72*, 57−62.

(6) Morita, S.; Fukase, M.; Hoshino, K.; Fukuda, Y.; Yamaguchi, M.; Morita, Y. Partial purification and characterization of a novel soybean protease which is inhibited by Kunitz and Bowman−Birk trypsin inhibitors. *J. Biochem.* (*Tokyo*) **1996**, *119*, 711−718.

(7) Kennedy, A. R. Chemopreventive agents: protease inhibitors. *Pharmacol. Ther.* **1998**, *78*, 167−209.

(8) Kennedy, A. R. The Bowman−Birk inhibitor from soybeans as an anticarcinogenic agent. *Am. J. Clin. Nutr.* **1998**, *68*, 1406S−1412S.

(9) Huang, C.; Ma, W.-Y.; Ryan, C. A.; Dong, Z. Proteinase inhibitors I and II from potatoes specifically block UV-induced activator protein-1 activation through a pathway that is independent of extracellular signal-regulated kinases, c-jun N-terminal kinases, and P38 kinase. *Proc. Natl. Acad. Sci. U.S.A.* **1997**, *94*, 11957−11962.

(10) Hill, A. J.; Peikin, S. R.; Ryan, C. A.; Blundell, J. E. Oral administration of proteinase inhibitor II from potatoes reduces energy intake in man. *Physiol. Behav.* **1990**, *48*, 241−246.

(11) Lisinska, G.; Leszczynski, W. *Potato Science and Technology*; Elsevier Applied Science: London, 1989.

(12) Pouvreau, L.; Gruppen, H.; Piersma, S. R.; van den Broek, L. A. M.; van Koningsveld, G. A.; Voragen, A. G. J. Relative abundance and inhibitory distribution of protease inhibitors in potato juice from cv. Elkana. *J. Agric. Food Chem.* **2001**, *49*, 2864−2874.

(13) Valueva, T. A.; Revina, T. A.; Mosolov, V. V. Potato tuber protein proteinase inhibitors belonging to the Kunitz soybean inhibitor family. *Biochemistry (Moscow)* **1997**, *62*, 1367−1374.

(14) Pouvreau, L.; Gruppen, H.; van Koningsveld, G. A.; van den Broek, L. A. M.; Voragen, A. G. J. The most abundant protease inhibitor in potato tuber (cv. Elkana) is a serine protease inhibitor from the Kunitz family. *J. Agric. Food Chem.* **2003**, *51*, 5001−5005.

(15) Bode, W.; Huber, R. Natural protein proteinase inhibitors and their interaction with proteinases. *Eur. J. Biochem.* **1992**, *204*, 433−451.

(16) Ingram, G. A. Lectins and lectin-like molecules in lower plants—I. Marine algae. *Dev. Comput. Immunol.* **1985**, *9*, 1−10.

(17) Ceciliani, F.; Bortolotti, F.; Menegatti, E.; Ronchi, S.; Ascenzi, P.; palmieri, S. Purification, inhibitory properties, amino acid sequence, and identification of the reactive site of a new serine proteinase inhibitor from oil-rape (*Brassica napus*) seed. *FEBS Lett.* **1994**, *342*, 221−224.

(18) Moses, E.; Hinz, H.-J. Basic pancreatic trypsin inhibitor has unusual thermodynamic stability parameters. *J. Mol. Biol.* **1983**, *170*, 765−776.

(19) De Jongh, H. H. J.; Goormaghtigh, E.; Killian, A. Analysis of circular dichroism spectra of oriented protein−lipid complexes: Toward a general application. *Biochemistry* **1994**, *33*, 14521−14528.

(20) Greenfield, N. J.; Fasman, G. D. Computed circular dichroism spectra for evaluation of protein conformation. *Biochemistry* **1969**, *8*, 4108−4116.

(21) Chang, C. T.; Wu, C.-S. C.; Yang, J. T. Circular dichroic analysis of protein conformation: Inclusion of the β-turns. *Anal. Biochem.* **1978**, *91*, 13−31.

(22) Hennessey, J. P.; Johnson, W. C. Information content in the circular dichroism of proteins. *Biochemistry* **1981**, *20*, 1085−1094.

(23) Pace, C. N.; Shirley, B. A.; Thomson, J. A. Measuring the thermal stability of a protein. In *Protein Structure*; *A Practical Approach*; Creighton, T. E., Ed.; IRL Press: Oxford, U.K., 1989.

(24) Haris, P. V.; Severcanb, F. FTIR spectroscopic characterization of protein structure in aqueous and non-aqueous media. *J. Mol. Catal.* **1999**, *7*, 207−221.

(25) De Meester, P.; Brick, P.; Lloyd, L. F.; Blow, D. M.; Onesti, S. Structure of the Kunitz-type soybean trypsin inhibitor (STI): implication for the interactions between members of the STI family and tissue-plasminogen activator. *Acta Crystallogr., Sect. D* **1998**, *54*, 589−597.

(26) Song, H. K.; Suh, S. W. Kunitz-type soybean trypsin inhibitor revisited: refined structure of its complex with porcine trypsin reveals an insight into the interaction between a homologous inhibitor from *Erythrina caffra* and tissue-type plasminogen activator. *J. Mol. Biol.* **1998**, *275*, 347−363.

(27) Goormaghtigh, E.; Cabiaux, V.; Ruysschaert, J.-M. Determination of soluble and membrane protein structure by Fourier transform infrared spectroscopy. III. Secondary structures. *Subcell. Biochem.* **1994**, *23*, 405−450.

(28) Tamura, A.; Kimura, K.; Takahara, H.; Akasaka, K. Cold denaturation and heat denaturation of *Streptomyces subtilisin* inhibitor. 1. CD and DSC studies. *Biochemistry* **1991**, *30*, 11307−11313.

(29) Boye, J. I.; Alli, I.; Ismail, A. A. Use of differential scanning calorimetry and infrared spectroscopy in the study of thermal and structural stability of α-lactalbumin. *J. Agric. Food Chem.* **1997**, *45*, 1116−1125.

(30) van Koningsveld, G. A.; Gruppen, H.; de Jongh, H. H. J.; Wijngaards, G.; van Boekel, M. A. J. S.; Walstra, P.; Voragen, A. G. J. The effects of pH and heat treatment on the structure and solubility of potato proteins in different preparations. *J. Agric. Food Chem.* **2001**, *49*, 4889−4897.

(31) Privalov, P. L. Stability of proteins. Small globular proteins. *Adv. Protein Chem.* **1979**, *33*, 167−241.

(32) Yamasaki, M.; Yano, H.; Aoki, K. Differential scanning calorimetric studies on bovine serum albumin: I. Effects of pH and ionic strength. *Int. J. Biol. Macromol.* **1990**, *12*, 263−268.

(33) Graziano, G.; Catanzano, F.; Barone, G. On the pH dependence of thermodynamic stability of α-maylase inhibitor Tendamistat. *Thermochim. Acta* **2000**, *345*, 59−66.

(34) Roychaudhuri, R.; Sarath, G.; Zeece, M.; Markwell, J. Reversible denaturation of the soybean Kunitz trypsin inhibitor. *Arch. Biochem. Biophys.* **2003**, *412*, 20−26.

(35) Teles, R. C. L.; de Souza, E. M. T.; de A. Calderon, L.; de Freitas, S. M. Purification and pH stability characterization of a chymotrypsin inhibitor from *Schizolobium parahyba* seeds. *Phytochemistry* **2004**, *65*, 793−799.

(36) Lehle, K.; Wrba, A.; Jaenicke, R. *Erythrina caffra* trypsin inhibitor retains its native structure and function after reducing its disulfide bonds. *J. Mol. Biol.* **1994**, *239*, 276−284.

(37) Kortt, A. A. Specificity and stability of the cymotrypsin inhibitor from winged bean seed (*Psophocarpus tetragonolobus* (L) Dc.). *Biochim. Biophys. Acta* **1981**, *657*, 212−221.

(38) Minuth, T.; Kramer, B.; Lehle, K.; Jaenicke, R.; Kohnert, U. The spectroscopic analysis, inhibition, and binding studies demonstrate the equivalence of *Erythrina caffra* trypsin inhibitor and the recombinant substitution variant recSerETI. *J. Biotechnol.* **1998**, *62*, 231−239.

(39) Tetenbaum, J.; Miller, L. M. A new spectroscopic approach to examining the role of disulfide bonds in the structure and unfolding of soybean trypsin inhibitor. *Biochemistry* **2001**, *40*, 12215−12219.

(40) Fukada, H.; Kitamura, S.; Takahashi, K. Calorimetric study of the thermal unfolding of Kunitz-type soybean trypsin inhibitor at pH 7.0. *Thermochim. Acta* **1995**, *266*, 365−372.

(41) Venyaminov, S. Y.; Yang, J. T. Determination of protein secondary structure. In *Circular Dichroism and the Conformational Analysis of Biomolecules*; Fasman, G. D., Ed.; Plenum Press: New York, 1996; pp 69−109.

(42) Manavalan, P.; Johnson, C. J. Variable selection method improves the prediction of protein secondary structure from circular dichroism spectra. *Anal. Biochem.* **1987**, *167*, 76−85.

(43) Wu, J.; Yang, J. T.; Wu, C.-S. C. β-II conformation of all β proteins can be distinguished from unordered form by circular dichroism. *Anal. Biochem.* **1992**, *200*, 359−364.

(44) Kidric, M.; Fabian, H.; Brzin, J.; Popovic, T.; Pain, R. H. Folding, stability, and secondary structure of a new cysteine dimeric proteinase inhibitor. *Biochem. Biophys. Res. Commun.* **2002**, *297*, 962−967.

(45) Sweet, R. M.; Wright, H. T.; Janin, J.; Chothia, C. H.; Blow, D. M. Crystal structure of the complex of porcine trypsin with soybean trypsin inhibitor (Kunitz) at 2.6-Å resolution. *Biochemistry* **1974**, *13*, 4212−4228.

(46) Menegatti, E.; Palmieri, S.; Walde, P.; Luisi, P. L. Isolation and characterization of a trypsin inhibitor from white mustard (*Sinapis alba* L.). *J. Agric. Food Chem.* **1985**, *33*, 784−789.

(47) Bonsager, B. C.; Praetorius-Ibba, M.; Nielsen, P. K.; Svensson, B. Purification and characterization of the β-trefoil protein barley α-amylase/subtilisin inhibitor overexpressed in *Escherichia coli*. *Protein Expr. Purif.* **2003**, *30*, 185−193.

(48) Lin, Y. H.; Chen, H. L. Level and heat stability of trypsin inhibitor activity among sweet potato (*Ipomoea batatas* LAm.) varieties. *Bot. Bull. Acad. Sin.* **1980**, *21*, 1−13.

(49) Vallée, F.; Kadziola, A.; Bourne, Y.; Juy, M.; Rodenburg, K. W.; Svensson, B.; Haser, R. Barley α-amylase bound to its endogenous protein inhibitor BASI: crystal structure of the complex at 1.9 Å resolution. *Structure* **1998**, *6*, 649−659.

(50) Venhudova, G.; Canals, F.; Querol, E.; Aviles, F. X. Mutations in the N- and C-terminal tails of potato carboxypeptidase inhibitor influence its oxidative refolding process at the reshuffling stage. *J. Biol. Chem.* **2001**, *276*, 11683−11690.

(51) Collen, D.; Lijnen, H. R. Molecular basis of fibrinolysis, as relevant for thrombolytic therapy. *Thromb. Haemost.* **1995**, *74*, 167−71.

Received for review April 15, 2004. Revised manuscript received September 16, 2004. Accepted September 24, 2004.

JF0493932